Combustion Explicitly Filtered Large-Eddy Simulation: A novel approach to multi-species LES

Ada Beroudiaux[⋆,+], Luc Vervisch[⋆], Quentin Cerutti[⋆], Pascale Domingo[⋆], Guillaume Ribert[⋆]
[⋆]CORIA-CNRS, INSA de Rouen Normandie, France
[+]SafranTech, Magny-Les-Hameaux, 78772, France

1 Introduction

In theory, Large-Eddy Simulation (LES) of combustion and flames involves filtering out high-frequency fluctuations while resolving low-frequency fluctuations using coarse computational meshes. In practice, this is achieved by introducing eddy viscosity to modify the flow's Reynolds number. While this approach is conceptually similar to steady Reynolds-Averaged Navier-Stokes (RANS) modeling, LES employs a lower level of additional viscosity to dampen only the smallest eddies. However, when applied to scalar fields, this methodology complicates the accurate representation of all transport phenomena, such as differential diffusion. As a result, there remains an inherent risk of over- or under-estimating the appropriate level of subgrid-scale viscosity. This issue is also particularly critical in high-speed flow simulations and detonations, where excessive viscosity can result in unphysical effects, such as the diffusion of heat through shock waves propagating upstream of reaction zones. An alternative strategy involves directly applying a regularization based on an explicit filtering operation to ensure that the scalar field remains resolved at the scale Δ [1]. A concept, previously explored in high-Schmidt-number flow simulations [2], is extended here to the context of flames. Furthermore, significant progress has been achieved in the mathematical development of constrained and optimization frameworks for the automated calculation of explicit forward and direct-inverse discrete filter coefficients tailored to a given filter transfer function [3]. This paper introduces a novel approach to LES of reactive flows by leveraging these filters to capture flame dynamics on computational grids coarser than the flame thickness.

2 Background

Let us consider a reactive scalar $\phi(\mathbf{x}, t)$ transported by a three-dimensional momentum field $\rho\mathbf{u}$, here ρ denotes the density and $\mathbf{u}$ is the velocity vector. The transport equation for ϕ takes the usual form:

$$\frac{\partial \rho\phi}{\partial t} + \nabla \cdot (\rho\mathbf{u}\phi + \mathbf{J}_\phi) = \dot{\omega}_\phi \, , \tag{1}$$

with $\mathbf{J}_\phi$ the molecular diffusion flux and $\dot{\omega}_\phi$ is a chemical source. This equation may also be written

$$\frac{\partial \rho\phi}{\partial t} + \nabla \cdot (\rho\mathbf{u}\phi) = -\rho V_\phi \mathbf{n} \cdot \nabla\phi = \rho V_\phi |\nabla\phi| \, , \tag{2}$$

with $\mathbf{n} = -\nabla\phi/|\nabla\phi|$ and $V_\phi = (-\nabla\cdot\mathbf{J}_\phi + \dot{\omega}_\phi)/(\rho|\nabla\phi|)$, the relative velocity to be added to the flow velocity $\mathbf{u}$ to follow the iso-scalar in its movement,

$$\frac{\partial\phi}{\partial t} + (\mathbf{u} + V_\phi\mathbf{n})\cdot\nabla\phi = 0\,. \tag{3}$$

Let us assume that the density and the velocity fields are known over a mesh that features a resolution of characteristic length $h > \eta_k$, with η_k the smallest of the flow characteristic length scales. The flow is determined from the solving of a close set of equations for $\overline{\rho}$ and $\widetilde{\mathbf{u}} = \overline{\rho\mathbf{u}}/\overline{\rho}$, where $\bar{\cdot}$ denotes quantities resolved at h by the mesh. Because of the stiff chemical source, gradients of ϕ will develop at scales smaller than h, leading to scalar signals that cannot be resolved by the coarse mesh.

The fluctuating scalar ϕ is decomposed into a low-frequency part $\widetilde{\phi} = \overline{\rho\phi}/\overline{\rho}$, resolved over the grid of size h, and a sub-grid (SGS), or high-frequency, part $\phi_{SGS} = \phi - \widetilde{\phi}$. The balance equation for the low-frequency part resolved by the mesh may be written:

$$\frac{\partial\overline{\rho}\widetilde{\phi}}{\partial t} + \nabla\cdot\left(\overline{\rho}\widetilde{\mathbf{u}}\widetilde{\phi} + \mathbf{J}_{\widetilde{\phi}}\right) = \dot{S}_{\widetilde{\phi}}\,, \tag{4}$$

where $\mathbf{J}_{\widetilde{\phi}}$ is the molecular diffusive flux of the resolved part of the signal. In practice, the RHS $\dot{S}_{\widetilde{\phi}}$ serves two objectives: (i) estimate $\overline{\dot{\omega}}_\phi$, the filtered chemical source, and (ii) diffuse the scalar field so that it can be resolved over the coarse mesh.

The exact expression for $\dot{S}_{\widetilde{\phi}}$ is obtained by applying a space filtering operation

$$\overline{\rho\phi}(x,t) = \int_{-\infty}^{+\infty} G_\Delta(s)\rho\phi(x-s,t)ds = \int_{-\infty}^{+\infty} G_\Delta(x-s)\rho\phi(s,t)ds\,, \tag{5}$$

to Eq. (1), where $G_\Delta(s)$ is a filter of characteristic size $\Delta > h$, then:

$$\dot{S}_{\widetilde{\phi}} = -\nabla\cdot\tau_\phi + \overline{\dot{\omega}}_\phi\,, \tag{6}$$

with τ_ϕ the SGS flux composed of the convective and molecular transport by unresolved fluctuations:

$$\tau_\phi = \tau_u + \tau_J = \left[\overline{\rho\mathbf{u}\phi} - \overline{\rho}\widetilde{\mathbf{u}}\widetilde{\phi}\right] + \left[\overline{\mathbf{J}_\phi} - \mathbf{J}_{\widetilde{\phi}}\right]\,, \tag{7}$$

Under a propagative form for the filtered scalar (Eq. (3)),

$$\frac{\partial\widetilde{\phi}}{\partial t} + \left(\widetilde{\mathbf{u}} + V^T_\phi\widetilde{\mathbf{n}}\right)\cdot\nabla\widetilde{\phi} = 0\,, \tag{8}$$

with $\widetilde{\mathbf{n}} = -\nabla\widetilde{\mathbf{n}}/|\nabla\widetilde{\mathbf{n}}|$ and

$$\overline{\rho}|\nabla\widetilde{\phi}|V^T_\phi = \overline{-\nabla\cdot\mathbf{J}_\phi + \dot{\omega}_\phi - \nabla\cdot\tau_u} = \overline{\rho V_\phi|\nabla\phi| - \nabla\cdot\tau_u}\,. \tag{9}$$

We now present an approach to solve Eq. (4), incorporating explicitly the filtering operation that eliminates scales smaller than Δ.

3 Explicitly filtered modeling

The flowchart of the model, which relies on relaxation toward filtered scalar fields resolved over a mesh of characteristic size h, is first introduced. In the next section, the underlying hypotheses of the modeling are further analyzed, before applying it to a bunsen H_2-Air flame with detailed chemistry and complex transport properties.

1. Let us first solve for the scalar fields (species mass fractions, temperature, energy, etc.) as if they were passive (non-reactive) and resolved by the mesh:

$$\frac{\partial \overline{\rho}\widetilde{\phi}}{\partial t} + \nabla \cdot \left(\overline{\rho}\widetilde{\mathbf{u}}\widetilde{\phi} + \mathbf{J}_{\widetilde{\phi}} \right) = 0 \, . \tag{10}$$

   This returns an intermediate solution field $\left[\overline{\rho}\widetilde{\phi}\right]^{\star}$. Because of the absence of a chemical source, Eq. (10) cannot generate very strong scalar gradients, only the convective part can steepen the distributions of scalars over the coarse mesh.

2. The solution of Eq. (10) is explicitly filtered to remove any high-frequency fluctuations developing at scales smaller than Δ over the mesh of resolution h:

$$\overline{\left[\overline{\rho}\widetilde{\phi}\right]^{\star}}(x,t) = \int_{-\infty}^{+\infty} G_{\Delta}(s) \left[\overline{\rho}\widetilde{\phi}(x-s,t)\right]^{\star} ds \, , \tag{11}$$

   where $G_{\Delta}(s)$ is the filtering operation.

3. To estimate the filtered chemical source, a deconvolution operation is applied to the vector of thermochemical scalars $\underline{\widetilde{\phi}}$:

$$\underline{\phi}^{+} = \mathcal{L}_{\Delta}^{-1}(\overline{\rho}\underline{\widetilde{\phi}})/\mathcal{L}_{\Delta}^{-1}(\overline{\rho}) \, . \tag{12}$$

   This deconvolution is performed inverting the Taylor expansion of the filter (Eq. (24)) and keeping only the second order term.

4. The characteristic filtering relaxation time scale, τ_{Δ}, is determined based on filter properties using a dynamic formulation or directly estimated from SGS quantities, such as SGS kinetic energy and flame parameters (discussed in more detail below).

$$\tau_{\Delta} = \mathcal{F}(M_{\Delta}, k_{SGS}^{1/2}, ...) \, . \tag{13}$$

5. The solution is relaxed towards the filtered field adding the chemical effects:

$$\overline{\rho}\widetilde{\phi}(t+\delta t) = \overline{\left[\overline{\rho}\widetilde{\phi}\right]^{\star}} + \left(\left[\overline{\rho}\widetilde{\phi}\right]^{\star} - \overline{\left[\overline{\rho}\widetilde{\phi}\right]^{\star}} \right) \exp\left(-\delta t/\tau_{\Delta}\right) + \delta t \times \overline{\dot{\omega}_{\phi}(\underline{\phi}^{+})} \, . \tag{14}$$

   In practice, this is equivalent to solving the closed balance equation:

$$\frac{\partial \overline{\rho}\widetilde{\phi}}{\partial t} + \nabla \cdot \left(\overline{\rho}\widetilde{\mathbf{u}}\widetilde{\phi} + \mathbf{J}_{\widetilde{\phi}} \right) = \frac{\overline{\overline{\rho}\widetilde{\phi}} - \overline{\rho}\widetilde{\phi}}{\tau_{\Delta}} + \overline{\dot{\omega}_{\phi}(\underline{\phi}^{+})} \, , \tag{15}$$

   in which the divergence of the SGS flux (Eq. (7)) is modeled with the linear relaxation $-\nabla \cdot \tau_{\phi} = (\overline{\overline{\rho}\widetilde{\phi}} - \overline{\rho}\widetilde{\phi})/\tau_{\Delta}$. This expression, which regularizes the scalar field at the scale Δ, is analogous to the linear mean-square estimation (LMSE/IEM) closure employed in probability density function (PDF) transport models to represent turbulent micro-mixing [4].

4 Dynamic formulation for the relaxation time

A dynamic formulation can be developed to determine the relaxation time toward the filtered values of the scalar field. The relaxation time scale, τ_Δ^ϕ, then depends on the species ϕ concerned. The SGS characteristic time can be estimated from the flow deformation as follows [5]:

$$\tau_\Delta^\phi = \frac{1}{C_\phi^2 |\nabla \widetilde{S}|} \ , \tag{16}$$

with $\widetilde{S} = \sqrt{2\widetilde{S}_{ij}\widetilde{S}_{ij}}$ and $\widetilde{S}_{ij} = 0.5(\partial \widetilde{u}_i/\partial x_j + \partial \widetilde{u}_j/\partial x_i)$. The modeled term (Eq. (7)) becomes

$$\nabla \cdot \tau_\phi = -C_\phi^2 |\nabla \widetilde{S}| \left(\overline{\overline{\rho}\widetilde{\phi}} - \overline{\rho}\widetilde{\phi} \right) \ . \tag{17}$$

Applying the dynamic procedure with a test filter $\widehat{\Delta} > \Delta$ [6, 7], the parameter C_ϕ reads

$$C_\phi^2 = -\frac{\nabla \cdot \mathcal{L}_\phi}{\mathcal{M}_\phi} \ , \tag{18}$$

with

$$\mathcal{L}_\phi = \widehat{\overline{\rho}\widetilde{\mathbf{u}}\widetilde{\phi}} - \widehat{\overline{\rho}}\widehat{\widetilde{\mathbf{u}}}\widehat{\widetilde{\phi}} + \widehat{\mathbf{J}}_{\widetilde{\phi}} - \mathbf{J}_{\check{\widetilde{\phi}}} \ , \tag{19}$$

$$\mathcal{M}_\phi = |\nabla \check{\widetilde{S}}| \left(\widehat{\widehat{\overline{\rho}}\check{\widetilde{\phi}}} - \widehat{\overline{\rho}}\check{\widetilde{\phi}} \right) - \widehat{|\nabla \widetilde{S}| \left(\overline{\overline{\rho}\widetilde{\phi}} - \overline{\rho}\widetilde{\phi} \right)} \ , \tag{20}$$

where $\check{\widetilde{\phi}} = \widehat{\overline{\rho}\widetilde{\phi}}/\widehat{\overline{\rho}}$. This dynamic procedure differs slightly from the usual formulation for scalar fluxes, as the relaxation toward the filtered value serves as a closure for the divergence of the flux rather than for the flux itself.

Applied to a set of species mass fractions Y_i, a corrective relaxation term

$$r_i^c = -\widetilde{Y}_i \sum_k \frac{\overline{\overline{\rho}\widetilde{Y}_k} - \overline{\rho}\widetilde{Y}_i}{\tau_\Delta^k} \ , \tag{21}$$

is added to Eq. (15) to secure mass conservation.

4 Analysis of explicitly filtered relaxation modeling

In Eq. (5), the density-weighted scalar signal can be expanded in Taylor series around $s = x$,

$$\rho\phi(s,t) = \sum_{n=0}^{\infty} \frac{(s-x)^n}{n!} \left.\frac{\partial^n \rho\phi}{\partial s^n}\right)_{s=x} \ . \tag{22}$$

The relation (5) into Eq. (22) leads to

$$\overline{\rho\phi}(x,t) = \sum_{n=0}^{\infty} \frac{(-1)^n}{n!} \left.\frac{\partial^n \rho\phi}{\partial s^n}\right)_{s=x} \int_{-\infty}^{+\infty} \xi^n G_\Delta(\xi) d\xi = \sum_{n=0}^{\infty} (-1)^n \left.\frac{\partial^n \rho\phi}{\partial s^n}\right)_{s=x} M_\Delta^n \ , \tag{23}$$

where M_Δ^n is the n-th moment of the filter G_Δ divided by $n!$. For symmetric filters, the odd moments vanish and one may write:

$$\overline{\rho}\widetilde{\phi} = \overline{\rho\phi} = \rho\phi + \sum_{n=1}^{\infty} \frac{\partial^{2n}\rho\phi}{\partial x^{2n}} M_\Delta^{2n} \,. \tag{24}$$

Introducing a relaxation time scale τ_Δ

$$\frac{\overline{\overline{\rho}\widetilde{\phi}} - \overline{\rho}\widetilde{\phi}}{\tau_\Delta} = \frac{1}{\tau_\Delta} \sum_{n=1}^{\infty} \frac{\partial^{2n}\overline{\rho}\widetilde{\phi}}{\partial x^{2n}} M_\Delta^{2n} \,, \tag{25}$$

$\dot{S}_{\widetilde{\phi}}$ (Eq. (6)) may then be written:

$$\dot{S}_{\widetilde{\phi}} = -\nabla \cdot \tau_\phi + \overline{\dot{\omega}}_\phi = \frac{M_\Delta^2}{\tau_\Delta} \frac{\partial^2 \overline{\rho}\widetilde{\phi}}{\partial x^2} + \mathcal{O}(\Delta^4) + \overline{\dot{\omega}}_\phi \,. \tag{26}$$

Link with eddy diffusivity transport: According to Eq. (26), the transport by the gradient hypothesis, $-\tau_\phi \approx \overline{\rho} D_T \nabla\widetilde{\phi}$, where $D_T \approx k_{SGS}^{1/2}\Delta$, acts as a regularization of the scalar field through a filtering operation truncated at fourth order. This is associated with the characteristic time scale:

$$\tau_\Delta \approx \frac{M_\Delta^2}{k_{SGS}^{1/2}\Delta} \,. \tag{27}$$

Link with thickened flame modeling: Similarly the thickened flame model (TFM) [8], in which the molecular diffusion coefficient D_ϕ (i.e., $-\mathbf{J}_\phi = \overline{\rho} D_\phi \nabla\widetilde{\phi}$) is augmented by a factor F to secure the resolution of the scalar over the mesh, would correspond to the application of a filtering operation such as:

$$\tau_\Delta \approx \frac{M_\Delta^2}{(F-1)D_\phi} \,. \tag{28}$$

To evaluate the accuracy of the proposed algorithm, which ensures precise control of the filtering operation, its ability to reproduce the asymptotic limit of a laminar flame propagating over coarse meshes is first tested (Fig. 1). The temperature equation is solved using single-step chemistry representative of methane-air combustion [9], with a laminar flame speed of $S_L = 0.38 \text{m}\cdot\text{s}^{-1}$. The source term is expressed as $\overline{\dot{\omega}}_\phi = \dot{\omega}(\widetilde{\phi})/F$, analogous to thickened flame modeling, with the thickening factor given here by $F(\tau_\Delta) = M_\Delta^2/(D_\phi \tau_\Delta) + 1$. Using M_Δ^2 from a Gaussian filter, the solution of Eq. (15) shows that the filtered flame propagates over coarse meshes with a deviation of only 0.02% from the laminar flame speed (results omitted for brevity). The numerical methods used in this analysis are consistent with those described in [9].

Link with SGS wrinkling modeling: Filtering the propagative form of the scalar equation (Eq. (3)) and combining with Eqs. (8) and (15) provides:

$$\overline{\rho} V_\phi^T |\nabla\widetilde{\phi}| = \overline{\rho V_\phi |\nabla\phi|} = -\nabla \cdot \mathbf{J}_{\widetilde{\phi}} + \frac{\overline{\overline{\rho}\widetilde{\phi}} - \overline{\rho}\widetilde{\phi}}{\tau_\Delta} + \overline{\dot{\omega}_\phi(\underline{\phi}^+)} \,. \tag{29}$$

In a premixed flame front, assuming a thin reaction zone, mass conservation imposes $\rho V_\phi = \rho_o S_L$, where S_L is the laminar flame consumption speed. Under this framework, $V_{\phi=0}^T$ becomes the so-called turbulent burning velocity S_T for ϕ a progress variable (0 in fresh gases and 1 in burnt gases), and $\Xi = \overline{|\nabla\phi|}/|\nabla\widetilde{\phi}| = S_T/S_L$ denotes the wrinkling factor. Then,

$$\begin{aligned} \tau_\Delta &= \frac{\overline{\overline{\rho}\widetilde{\phi}} - \overline{\rho}\widetilde{\phi}}{\mathcal{D}} \\ \mathcal{D} &= \rho_o S_L \Xi |\nabla\widetilde{\phi}| + \nabla \cdot (\mathbf{J}_{\widetilde{\phi}}) - \overline{\dot{\omega}_\phi(\underline{\phi}^+)} \,. \end{aligned} \tag{30}$$

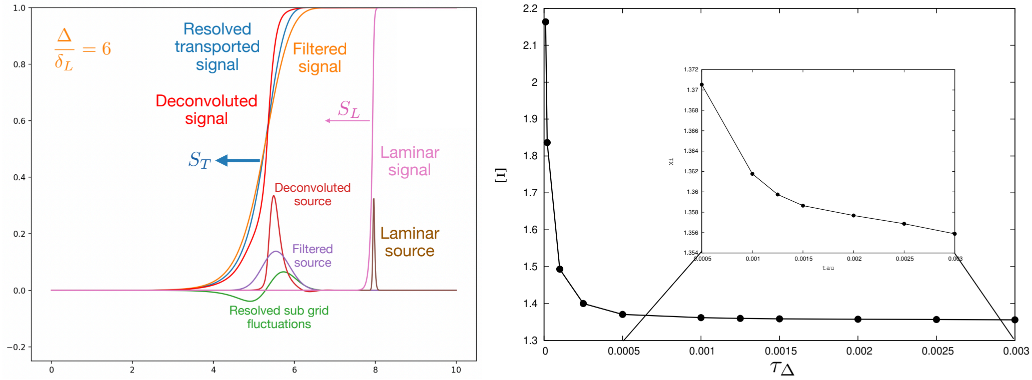

(a) 1D-filtered flame. (b) $\Xi = \Xi(\tau_\Delta)$

Figure 1: (a) 1D-filtered flame with SGS effects. δ_L: laminar flame thickness. Domain length is $80\delta_L$. $\Delta = 6\delta_L$. $\tau_\Delta = 10h^2/D_\phi$. (b) Response of SGS wrinkling Ξ vs. τ_Δ for $\Delta = 2\delta_L$ with zoom for $\tau_\Delta \in [5 \cdot 10^{-4}, 3 \cdot 10^{-3}]$.

In a second preliminary test, Eq. (15) is solved to simulate a filtered one-dimensional flame, with sub-grid scale (SGS) effects modeled through the relaxation term, $(\overline{\overline{\rho}\widetilde{\widetilde{\phi}}} - \overline{\rho}\widetilde{\phi})/\tau_\Delta$. A Gaussian filter is applied, and here the Van-Cittert algorithm [10] is used for deconvolution to compute the chemical source term (single-step model, as in previous test). Figure 1(a) presents representative profiles of the model components alongside the reference laminar flame. The resulting SGS wrinkling, computed as S_T/S_L, is plotted against τ_Δ in Fig. 1(b). In the practice of three-dimensional simulations, advanced dynamic modeling of Ξ [11] will provide a closure for τ_Δ through Eq. (30). Moreover, as discussed above, Eq. (15) offers a versatile framework applicable to various combustion models, contingent on the selection of τ_Δ.

5 Multispecies bunsen flame burner simulation

Both direct numerical simulation (DNS) and large eddy simulation (LES) were performed for a Bunsen-premixed stoichiometric hydrogen-air flame diluted with H_2O. The numerical methods, detailed chemistry, and transport properties used follow those described in [12], with computational details given in Fig. 2. At the same physical instant in time, the LES following the explicitly filtered methodology successfully captures the flame dynamics observed in the DNS, including the presence of intermediate radicals such as H_2O_2.

References

[1] A. Bertles, B. Kober, A. Rittler, and A. Kempf, "Large-eddy simulation of Sandia flame D with efficient explicit filtering," *Flow Turbul. Combust.*, vol. 102, pp. 887–907, 2019.

[2] M. Leer, M. W. A. Pettit, J. T. Lipkowicz, P. Domingo, L. Vervisch, and A. M. Kempf, "A conservative Euler-Lagrange decomposition principle for the solution of multi-scale flow problems at high schmidt or prandtl numbers," *J. Comput. Phys.*, vol. 464, p. 111216, 2022.

[3] Z. Nikolaou, L. Vervisch, and P. Domingo, "An optimisation framework for the development of explicit discrete forward and inverse filters," *Comput. Fluids*, no. 255, p. 105840, 2023.

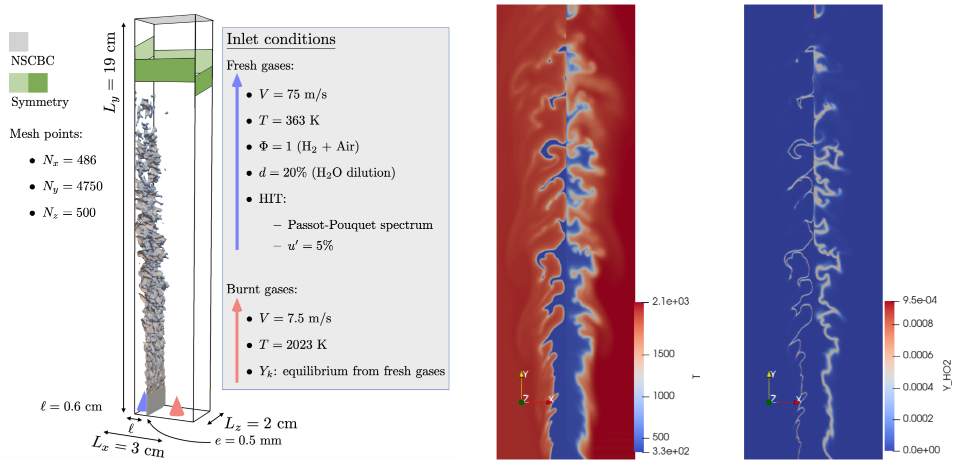

(a) Computational domain - DNS (b) Temp. Left: DNS. Right: LES. (c) HO_2. Left: DNS. Right: LES.

Figure 2: Busen H_2-Air flame. LES: $\Delta = 500\mu$m. $\tau_\Delta = M_\Delta^2/(k_{SGS}^{1/2}\Delta)$.

[4] C. Dopazo and E. O'Brien, "Functional formulation of nonisothermal turbulent reactive flows," *Phys. Fluids*, vol. 17, pp. 1968–1975, 1974.

[5] J. Smagorinsky, "General circulation experiments with the primitives equations," *Mon. Weather Rev.*, vol. 61, pp. 99–164, 1963.

[6] M. Germano, "Turbulence: The filtering approach," *J. Fluid Mech.*, vol. 238, pp. 325–336, 1992.

[7] S. Ghosal, T. S. Lund, P. Moin, and K. Akselvoll, "A dynamic localization model for large-eddy simulation of turbulent flows," *J. Fluid Mech.*, vol. 286, p. 229, 1995.

[8] O. Colin, F. Ducros, D. Veynante, and T. Poinsot, "A thickened flame model for Large Eddy Simulations of turbulent premixed combustion," *Physics of Fluids*, vol. 12, no. 7, pp. 1843–1863, 2000.

[9] P. Domingo and L. Vervisch, "Large Eddy Simulation of premixed turbulent combustion using approximate deconvolution and explicit flame filtering," *Proc. Combust. Inst.*, vol. 35, no. 2, pp. 1349–1357, 2015.

[10] P. H. van Cittert, "Zum Einfluß der Spaltbreite auf die Intensitätsverteilung in Spektrallinien. II," *Zeitschrift fur Physik*, vol. 69, no. 5-6, pp. 298–308, May 1931.

[11] S. Puggelli, D. Veynante, and R. Vicquelin, "Impact of dynamic modelling of the flame subgrid scale wrinkling in large-eddy simulation of light-round in an annular combustor," *Combustion and Flame*, vol. 230, p. 111416, 2021.

[12] G. Ribert, P. Domingo, and L. Vervisch, "Analysis of sub-grid scale modeling of the ideal-gas equation of state in hydrogen-oxygen premixed flames," *Proc. Combust. Inst*, vol. 37, pp. 2345–2351, 2019.